

## Probing Spatial Spin Correlations of Ultracold Gases by Quantum Noise Spectroscopy

G. M. Bruun,<sup>1,2</sup> Brian M. Andersen,<sup>2</sup> Eugene Demler,<sup>3</sup> and Anders S. Sørensen<sup>2,4</sup>

<sup>1</sup>*Dipartimento di Fisica, Università di Trento and CNR-INFM BEC Center, I-38050 Povo, Trento, Italy*

<sup>2</sup>*Niels Bohr Institute, University of Copenhagen, DK-2100 Copenhagen Ø, Denmark*

<sup>3</sup>*Department of Physics, Harvard University, Cambridge, Massachusetts 02138, USA*

<sup>4</sup>*QUANTOP-Danish Quantum optics center, Niels Bohr Institute, DK-2100 Copenhagen Ø, Denmark*

(Received 1 September 2008; published 20 January 2009)

Spin noise spectroscopy with a single laser beam is demonstrated theoretically to provide a direct probe of the spatial correlations of cold fermionic gases. We show how the generic many-body phenomena of antibunching, pairing, antiferromagnetic, and algebraic spin liquid correlations can be revealed by measuring the spin noise as a function of laser width, temperature, and frequency.

DOI: 10.1103/PhysRevLett.102.030401

PACS numbers: 03.75.Ss, 03.75.Hh, 05.30.Fk, 05.40.Ca

Ultracold atoms offer the possibility to prepare, manipulate, and probe paradigm phases of strongly correlated systems. Considerable efforts are devoted to develop sensitive detection schemes to study these phases. Whereas most experiments are based on measuring mean values of various observables, further insight can be obtained from the correlations in the noise of the atomic distribution [1–3]. In recent experiments, a new technique using phase contrast imaging was used to probe the spin of ultracold atoms [4,5]. In related experiments [6–8], similar techniques have been pushed to the point where they are sensitive to the quantum fluctuations of the atoms. In this Letter, we show that quantum spin noise spectroscopy along the lines of Refs. [4–8] constitutes a sensitive probe of the correlations of the underlying quantum state. We focus on generic many-body phenomena such as antibunching, pairing, and spin liquids. Furthermore, we show that spin noise measurement is an ideal tool for probing antiferromagnetic ordering and phase transitions for atoms in optical lattices, which is currently a main challenge in cold atoms physics. Related theoretical studies of spin noise have been presented in Refs. [9–11].

Quantum noise limited probing of the spin state may be obtained either by polarization rotation [6,7] or phase contrast imaging [8,12]. In the first approach, the spin imprints a phase shift on a laser beam, which is subsequently measured by interfering the beam with another laser beam (i.e., homodyne detection). In the polarization rotation measurement, the two laser beams are replaced by two different polarization modes, making the setup less sensitive to fluctuations in optical path length and beam profile. We explore the situation where a laser beam is passed through the sample and the final result is measured by photo detectors. In the limit of strong beams (many photons) experiencing a small phase change, the observable, i.e., the measured light quadrature in the homodyne detection, may be expressed as [7,12–14]

$$\hat{X}_{\text{out}} = \hat{X}_{\text{in}} + \frac{\kappa}{\sqrt{2}} \hat{M}_z. \quad (1)$$

Here,  $\hat{X}_{\text{in/out}}$  is a canonical position operator describing the light normalized such that the input corresponds to vacuum noise  $\langle \hat{X}_{\text{in}}^2 \rangle = 1/2$ , and  $\kappa$  is a coupling constant. The effective measured atomic operator is  $\hat{M}_z = \int d^3r \phi(\mathbf{r}) \hat{s}_z(\mathbf{r}) / \sqrt{A}$ , where  $A = \int d^3r \phi^2(\mathbf{r}) n(\mathbf{r}) / 4$  is a normalization constant,  $\phi(\mathbf{r})$  is the spatial intensity profile of the laser beam, and  $\hat{s}_z(\mathbf{r}) = [\hat{\psi}_{\uparrow}^\dagger(\mathbf{r}) \hat{\psi}_{\uparrow}(\mathbf{r}) - \hat{\psi}_{\downarrow}^\dagger(\mathbf{r}) \hat{\psi}_{\downarrow}(\mathbf{r})] / 2 = [\hat{n}_{\uparrow}(\mathbf{r}) - \hat{n}_{\downarrow}(\mathbf{r})] / 2$  gives the local population imbalance (magnetization) with  $\hat{\psi}_{\sigma}(\mathbf{r})$  being the atomic field operator. We consider a two-component atomic gas ( $\sigma = \uparrow, \downarrow$ ) with total local density  $n(\mathbf{r}) = \langle \hat{n}_{\uparrow}(\mathbf{r}) + \hat{n}_{\downarrow}(\mathbf{r}) \rangle$  and assume Gaussian laser profiles  $\phi(\mathbf{r}) \propto e^{-(x^2+y^2)/d^2}$ . By measuring the observable  $\hat{X}_{\text{out}}$ , it is possible to obtain spatially resolved information about the magnetization  $\langle \hat{X}_{\text{out}} \rangle = \kappa \langle \hat{M}_z \rangle / \sqrt{2}$ . In many cases, however, interesting states may not have any net magnetization  $\langle \hat{M}_z \rangle = 0$ . In this Letter, we will only consider such situations and show that a measurement of the quantum noise  $\langle \hat{X}_{\text{out}}^2 \rangle = (1 + R\kappa^2) / 2$ , where  $R \equiv \langle \hat{M}_z^2 \rangle$  giving

$$R = \frac{1}{A} \int d^3r_1 d^3r_2 \phi(\mathbf{r}_1) \phi(\mathbf{r}_2) \langle \hat{s}_z(\mathbf{r}_1) \hat{s}_z(\mathbf{r}_2) \rangle \quad (2)$$

provides insight into the state of the system. Since  $R$  is quadratic in the atomic density operators, it gives a direct measure of the atomic correlations in the system. The normalization in Eq. (2) is chosen such that the quantum noise of an uncorrelated state, where each atom has an equal probability of being in each of the two internal states, is  $R = 1$  (standard quantum limit).

We first consider the normal phase, where the spin fluctuations have a length scale of  $k_F^{-1}$ . It follows that  $R$  vanishes if the effective volume  $V_B = (\int_V d^3r \phi)^2 / \int_V d^3r \phi^2$  is large,  $V_B \gg k_F^{-3}$ . Fermi statistics thus suppresses the noise below the standard quantum limit  $R = 1$ . For a finite laser beam, there will, however, be a noise contribution from the boundary  $\langle M_z^2 \rangle \sim d$ , which translate into  $R \sim 1/k_F d$ .

A key property of pairing is that the two particle density matrix  $\langle \psi_{\uparrow}^{\dagger}(\mathbf{r}_1)\psi_{\downarrow}^{\dagger}(\mathbf{r}_2)\psi_{\downarrow}(\mathbf{r}'_2)\psi_{\uparrow}(\mathbf{r}'_1) \rangle$  has a macroscopic eigenvalue  $p_c N$  with  $N$  the number of particles and  $p_c$  the condensate fraction. Spin noise spectroscopy probes the two particle density matrix directly, and in the large  $d$  limit, the noise is dominated by the largest eigenvalue  $p_c N$ . The noise depends on the shape of the applied laser beam: assuming a laser profile with a radius  $d$  and sharp edges compared to the radius  $\xi$  (coherence length) of the pair wave function  $\chi(\mathbf{r})$ , the noise is proportional to the number of pairs within  $\xi$  of the edge such that only one particle is inside the beam. This gives a scaling  $R \propto 1/d$  as in the normal case. With a smooth laser profile with radius  $d$  and fall-off distance  $D > \xi$ , the noise is due to pairs in the edge region. These pairs couple to the gradient ( $\sim 1/D$ ), and the noise from the difference in signal from  $\uparrow$  and  $\downarrow$  particles is  $\sim \int d^3 r \chi^2(r) r^2 / D^2 \sim \xi^2 / D^2$ . This should be multiplied by the number of pairs in the edge region  $\sim L_z d D p_c N / V$ , where  $L_z$  ( $V$ ) denotes the length (volume) of the system. Since  $A \sim L_z d^2 N / V$ , we get  $R \sim p_c \xi^2 / D d$ . With a Gaussian beam  $D \sim d$ , and the scaling  $R \sim p_c \xi^2 / d^2$  thus provides a measurement of  $\xi$  and  $p_c$ .

We now use the BCS wave function to derive this scaling rigorously in the BCS and BEC limits. Consider a homogeneous gas with constant density  $n_{\sigma}(\mathbf{r}) = N_{\sigma} / V$ . Wick's theorem yields  $\langle \hat{s}_z(\mathbf{r}_1)\hat{s}_z(\mathbf{r}_2) \rangle = n\delta(\mathbf{r}) - 2\theta^2(r) - 2F^2(r)$  with  $\mathbf{r} = \mathbf{r}_1 - \mathbf{r}_2$ ,  $\theta(r) = \langle \hat{\psi}_{\sigma}^{\dagger}(\mathbf{r}_1)\hat{\psi}_{\sigma}(\mathbf{r}_2) \rangle$ , and  $F(r) = \langle \hat{\psi}_{\uparrow}(\mathbf{r}_1)\hat{\psi}_{\downarrow}(\mathbf{r}_2) \rangle$ . We then find

$$R = 1 - \frac{2}{A} \int d^3 r_1 d^3 r_2 \phi(\mathbf{r}_1)\phi(\mathbf{r}_2)[\theta^2(r) + F^2(r)]. \quad (3)$$

In the BEC regime  $k_F a \rightarrow 0_+$ , the chemical potential is  $\mu \rightarrow -\hbar^2/2ma^2$ . This gives  $u_k v_k \rightarrow \Delta/2(|\mu| + k^2/2m)$  and  $v_k^2 \rightarrow \Delta^2/4(|\mu| + k^2/2m)^2$  for the coherence factors defined as  $u^2 = (1 + \xi/E)/2$ ,  $v^2 = 1 - u^2$  with  $E = (\xi^2 + \Delta^2)^{1/2}$  and  $\xi = k^2/2m - \mu$ . We obtain  $\theta(r)/n_{\sigma} = \exp(-r/a)$  and  $F(r)/n_{\sigma} = \sqrt{3\pi/k_F a} \exp(-r/a)/k_F r$  which is proportional to the asymptotic bound state wave function for a potential with scattering length  $a$ . Likewise, in the BCS limit  $k_F a \rightarrow 0_-$ ,  $\theta(r)/n_{\sigma} = 3[\text{sinc}k_F r - k_F r \text{cos}k_F r \sqrt{\pi r/2\xi} \exp(-r/\xi)]/(k_F r)^3$  and  $F(r)/n_{\sigma} = 3 \text{sinc}k_F r \sqrt{\pi/2\xi r} \exp(-r/\xi)/k_F^2 r$  for  $r \rightarrow \infty$  where  $\xi = k_F/m\Delta$  ( $\hbar = 1$ ) and  $\Delta$  is the gap. Using these limiting forms in (3), we obtain for  $d \rightarrow \infty$

	Normal phase	BCS limit	BEC limit
$R(d)$	$\frac{3\pi^{1/2}}{2^{5/2}} \frac{1}{k_F d}$	$\frac{\xi}{4k_F d^2}$	$\frac{a^2}{6d^2}$

For  $s$ -wave interactions, the pair wave function has a short-range divergence (bunching) given by  $F(r) = m\Delta/4\pi r$  [15] resulting in a linear decrease of the noise for  $k_F d \rightarrow 0$ . Using  $p_c \sim 1/k_F \xi$ , the BCS result agrees with the estimate given in the previous section.

In Fig. 1, we plot  $R(d)$  for a homogeneous system of transverse radius  $L = 100k_F^{-1}$  at  $T = 0$ . Results for the

normal phase and the superfluid phase with  $(k_F a)^{-1} = -1$  (BCS regime),  $(k_F a)^{-1} = 0$  (unitary limit), and  $(k_F a)^{-1} = 2$  (BEC regime) are shown. The noise is calculated numerically from (3) using the BCS wave function. The noise is *below* the quantum limit  $R \leq 1$  and  $R \rightarrow 0$  for  $d \rightarrow \infty$  in agreement with the analysis above. Pairing suppresses the noise compared to the normal state due to positive correlations between opposite spin states. The suppression increases with the pairing moving toward the BEC side.

For large  $d$ , the laser probes a significant fraction of the system, and it is important to include possible spin fluctuations due to the experimental preparation of the system. Such fluctuations will be limited by the standard quantum limit, i.e.,  $R = \beta$  with  $\beta \gtrsim 1$  when probing the entire system. When probing a subsystem, this gives an extra contribution  $\sim \beta V_B/V$  which is important for large  $d$  for the normal phase and the superfluid phase on the BEC side  $(k_F a)^{-1} = 2$  (see inset in Fig. 1). However, this term is absent for  $(k_F a)^{-1} \lesssim 0.5$  since superfluidity quenches spin noise in this regime [16–18]. Observing  $R \ll 1$  for a large portion of the sample would represent an extreme experimental demonstration of this quenching.

The observed enhancement of the nuclear spin relaxation just below the transition temperature  $T_c$  (Hebel-Slichter effect) constitutes one of the hallmark experimental tests of BCS theory. We now demonstrate the existence of a spin noise spectroscopy analogy to the Hebel-Slichter effect. Similar effects have been demonstrated to occur in inelastic light scattering and Bragg scattering experiments [19]. The probing technique discussed in this Letter is in principle nondestructive. By recording the signal for a long duration of time, one can thus obtain all frequency components of the noise  $R(d, \omega)$  [10]; i.e., Fourier transforming of the measured  $\hat{X}_{\text{out}}(t)$  provides a measurement of

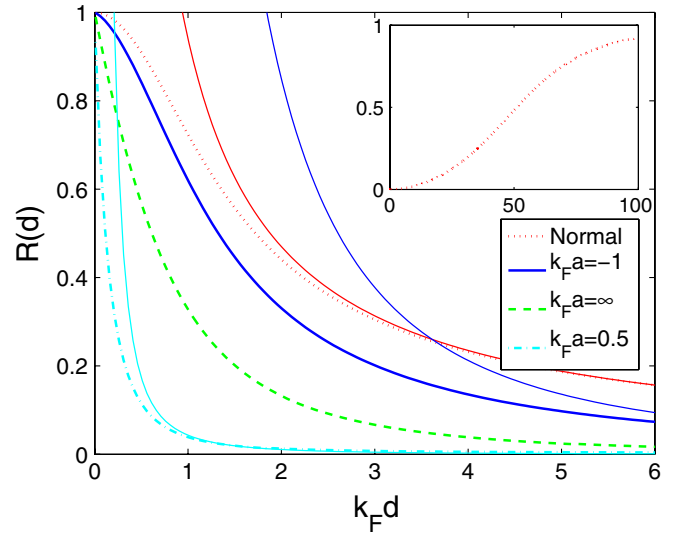


FIG. 1 (color online). Noise  $R(d)$  for various coupling strengths. The thin lines show the  $d \rightarrow \infty$  limit (see Table). The inset shows the large  $d$  behavior  $d/L \sim \mathcal{O}(1)$  with  $\beta = 1$  for the normal phase and the superfluid phase in the BEC limit.

$M_z(\omega)$ . Such probing will have similar signal-to-noise ratio  $\kappa^2(\omega) \sim \eta\alpha$ , but since spontaneous emission may lead to significant heating,  $\eta$  may have to be kept very low to avoid the system heating up. Using (3), we obtain

$$R(d, \omega) = \frac{8\pi m d^2}{n} \int \frac{d^3 k}{(2\pi)^3} \frac{E'}{\sqrt{E'^2 - \Delta^2}} (uu' + vv')^2 \times f(1 - f') e^{-(\mathbf{k}_\perp - \mathbf{k}'_\perp)^2 d^2 / 2} I_0(k_\perp k'_\perp d^2) \quad (4)$$

where  $I_0$  is the modified Bessel function of the first kind,  $\mathbf{k}_\perp = (k_x, k_y)$  is the transverse momentum, and  $f = [\exp(\beta E) + 1]^{-1}$ . The primed quantities refer to the momentum  $\mathbf{k}'$  with energy  $E' = E + \omega$ . There is momentum conservation along the  $z$ -direction with  $k'_z = k_z$  whereas  $\mathbf{k}'_\perp \neq \mathbf{k}_\perp$  due to the transverse Gaussian profile. Equation (4) gives the noise contribution from quasiparticle scattering from momentum  $\mathbf{k}$  to  $\mathbf{k}'$ . There are additional terms describing pair breaking and quasiparticle absorption which do not affect the Hebel-Slichter effect.

In Fig. 2, we plot  $R(d, \omega)$  as a function of  $T/T_c$  calculated numerically from (4) using the self consistently determined gap  $\Delta(T)$ . We have chosen  $k_F a = -1$  giving  $T_c/T_F \approx 0.13$  and  $\omega/k_B T_c = 0.08$  since the Hebel-Slichter effect only occurs for  $\omega \lesssim k_B T_c$ . For narrow laser widths, a Hebel-Slichter peak is prominent below  $T_c$ . It decreases with increasing  $d$  and disappears for  $d \gg \xi(T = 0) \approx 9$ . This is because for large laser widths, the scattering becomes subject to momentum conservation which restricts the available phase space.

Quantum systems in periodic potentials constitute another class of intriguing systems which can be examined by cold atomic gases using optical lattices. Superfluidity in lattices, possibly of  $d$ -wave symmetry, can be detected by suppression of spin noise similar to the discussion above for homogeneous systems. One could use a laser with

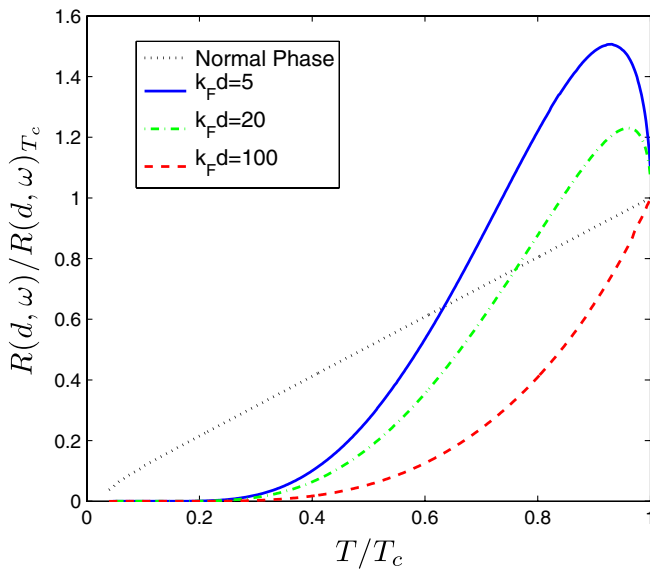


FIG. 2 (color online).  $R(d, \omega)$  in units of  $R(d, \omega)$  at  $T_c$  for various laser widths  $d$  and  $k_F a = -1$ .

elliptical transverse profile to detect the anisotropic suppression of spin noise due to the  $d$ -wave symmetry.

Presently, a main experimental goal in optical lattices is to observe the onset of antiferromagnetic (AFM) correlations with decreasing temperature [20]. As demonstrated below, spin noise spectroscopy can measure the magnetic susceptibility and hence constitutes an important experimental probe of the spin correlations. As an example, we study atoms described by the Hubbard model which in the strong repulsion limit at half filling for  $kT \ll U$  reduces to the AFM Heisenberg model,  $H = J \sum_{\langle i, j \rangle} \mathbf{s}_i \cdot \mathbf{s}_j$ , where  $\langle i, j \rangle$  denotes nearest-neighbor pairs and  $\mathbf{s}_i$  is the spin 1/2 operator for the atoms at site  $i$ . Assuming, without loss of generality, a staggered magnetization along the  $z$ -direction, we now show how to detect AFM correlations by measuring  $R_{\parallel} \equiv \langle \hat{M}_z^2 \rangle$  and  $R_{\perp} \equiv \langle \hat{M}_x^2 \rangle$ , where  $M_x$  is defined analogous to  $M_z$ . (A preferred direction for the broken symmetry can be induced by enforcing a slight anisotropy in the exchange coupling  $J$ .) We are mainly interested in the  $T$  dependence and focus on the situation where we probe the entire ensemble. Therefore, we assume a broad laser profile with  $\phi = 1$  in (2) such that  $R_{\parallel(\perp)} = 4 \langle S_{z(x)} S_{z(x)} \rangle / N$  with  $\mathbf{S} = \sum_i \mathbf{s}_i$  and  $N$  is the number of spins. In the paramagnetic phase,  $R_{\parallel} = R_{\perp} = 4kT\chi$  where  $\chi$  is the magnetic susceptibility. A high  $T$  expansion yields for the 2D square and 3D cubic lattices [21]

$$4kT\chi = \begin{cases} 1 - 2x + 2x^2 - 1.333x^3 + \dots, & 2D \\ 1 - 3x + 6x^2 - 11x^3 + \dots, & 3D \end{cases} \quad (5)$$

where  $x = J/2kT$ . In 2D, the system remains paramagnetic for  $T > 0$ , and modified spin-wave theory yields  $\chi = (12J)^{-1} [0.524 + 0.475T/J + \mathcal{O}(T^3)]$  for  $T/J \ll 1$  [22]. In the 3D case, the system undergoes a phase transition to an AFM phase at the Néel temperature  $T_N$ . In the AFM phase,  $R_{\parallel} \neq R_{\perp}$ . Using spin-wave theory for  $T < T_N$ , we obtain  $R_{\perp} = kT/(3J)$  and

$$R_{\parallel} = \frac{4}{N} \sum_{\mathbf{k}} \frac{1}{2 \sinh^2(\beta \omega_{\mathbf{k}}/2)}. \quad (6)$$

Here,  $\omega_{\mathbf{k}} = 3J\sqrt{1 - \gamma_{\mathbf{k}}^2}$  is the spin-wave energy with  $\gamma_{\mathbf{k}} = (\cos k_x a + \cos k_y a + \cos k_z a)/3$  for a cubic lattice with lattice constant  $a$ . The sum in (6) is over the reduced Brillouin zone. For  $kT \ll J$ , (6) yields  $R_{\parallel} = 4(kT)^3/(3s^3)$ , with  $s = \sqrt{3}J$  the spin-wave velocity. As shown in Fig. 3, the onset of AFM correlations in the paramagnetic phase can be detected as a decrease in the noise from the uncorrelated result  $R_{\parallel} = R_{\perp} = 1$  as described by (5). By comparing with the high  $T$  expansion, the spin noise may even serve as an accurate thermometer for the spin temperature. Furthermore, the AFM phase for the 3D case can be detected by observing  $R_{\parallel} \neq R_{\perp}$ . An advantage of probing collective operators like  $S_z$  is that they are conserved, and therefore could be measured after time of flight. In this case, however, care has to be taken of the contribution from

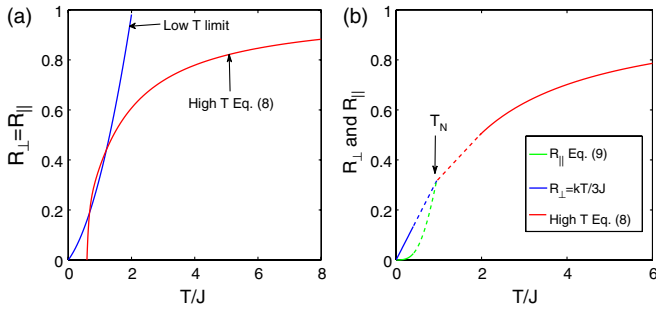


FIG. 3 (color online).  $R_{\parallel}$  and  $R_{\perp}$  for a 2D (a) and 3D (b) system. Solid lines are the high and low  $T$  results discussed in the text and the dashed lines in (b) (obtained by simple rescaling) indicate how they meet at  $T_N \approx 0.946J$  [27].

the boundary. We do not expect the trapping potential to change these results qualitatively [23,24].

The method presented here can also be used to probe the correlations of more exotic quantum phases such as resonating valence bond states and algebraic spin liquids [25]. These states are characterized by long-range spin correlations  $\langle \mathbf{s}(\mathbf{r})\mathbf{s}(0) \rangle \sim (-1)^{r_x+r_y}/r^{(1+\eta)}$ . Techniques exist for addressing, e.g., every second site in a lattice [26]. Flipping every second spin before the measurement [ $s_z \rightarrow (-1)^{r_x+r_y}s_z$ ] will give  $\langle s_z(\mathbf{r})s_z(0) \rangle \sim 1/r^{(1+\eta)}$ . Performing noise spectroscopy on this state will give a contribution from the long-range correlations  $R \sim d^{(1-\eta)}$ . By measuring the scaling of  $R$  with  $d$ , one can thus determine  $\eta$ .

Finally, we consider the experimental requirements for realizing our scheme. The experiments should be quantum noise limited with all classical noise sources suppressed. This has already been achieved in several experiments [6–8,12], and we expect it to be simpler to realize for the smaller systems considered here. In addition, the atomic noise should be large compared to the light noise inherently present in the probe. The spontaneous emission probability pr. atom caused by the probing light is  $\eta \sim \kappa^2/\alpha$ , where  $\alpha = 3nL_z\lambda^2\gamma_x/\gamma 2\pi$  is the optical depth of the ensemble [7,12,13]. Taking  $n \sim 10^{12} \text{ cm}^{-3}$ ,  $L_z \sim 100 \mu\text{m}$ , a probing wavelength  $\lambda = 671 \text{ nm}$  corresponding to Li, and a branching ratio  $\gamma_x/\gamma = 1/2$  gives  $\alpha = 16$  for a harmonically trapped Fermi gas. For atoms in optical lattices at half filling,  $\alpha \approx N_s = 50$  where  $N_s$  is the number of lattice sites in each direction. One can thus have a large signal-to-noise ratio  $\kappa^2 R \gtrsim 1$  with very little noise added from spontaneous emission during the probing  $\eta = \kappa^2/\alpha \ll 1$ . Another concern is the spatial resolution. Experimentally, one may obtain a resolution down to  $d \sim 5\lambda$  [4]. Taking  $n \sim 10^{12} \text{ cm}^{-3}$ , this corresponds to  $k_F d \sim 10$ . Thus, it may require an adiabatic expansion of the gas to observe the small scale limit of Fig. 1. However, it is possible directly to observe the large  $d$  scaling, the Hebel-Slichter effect, and the onset of magnetic correlations.

In summary, we have shown how to extract the correlations of quantum states of ultracold atoms using spin noise spectroscopy. This was demonstrated explicitly by calcu-

lating the spin noise for normal Fermi gases, superfluids, paramagnetic and AFM phases and algebraic spin liquids. This method can be applied to other strongly correlated systems as well as extended to higher order moments [11]. It may even be extended to full quantum state tomography of the two particle density matrix.

We acknowledge useful conversations with R. Cherng, E. Polzik, A. Sanpera. Partial support was provided by the Villum Kann Rasmussen Foundation (B. M. A.) and the Harvard-MIT CUA, DARPA, MURI, and the NSF Grant No. DMR-0705472 (E. D.).

- [1] E. Altman, E. Demler, and M. Lukin, Phys. Rev. A **70**, 013603 (2004).
- [2] S. Fölling *et al.*, Nature (London) **434**, 481 (2005); M. Greiner *et al.*, Phys. Rev. Lett. **94**, 110401 (2005).
- [3] S. Hofferberth *et al.*, Nature Phys. **4**, 489 (2008); I. B. Spielman, W. D. Phillips, and J. V. Porto, Phys. Rev. Lett. **98**, 080404 (2007); V. Guarrera *et al.*, *ibid.* **100**, 250403 (2008); Z. Hadzibabic *et al.*, *ibid.* **93**, 180403 (2004).
- [4] Y. Shin *et al.*, Phys. Rev. Lett. **97**, 030401 (2006).
- [5] L. E. Sadler *et al.*, Nature (London) **443**, 312 (2006).
- [6] J. L. Sørensen, J. Hald, and E. S. Polzik, Phys. Rev. Lett. **80**, 3487 (1998).
- [7] J. Sherson, B. Julsgaard, and E. S. Polzik, Adv. At. Mol. Opt. Phys. **54**, 81 (2006).
- [8] P. J. Windpassinger *et al.*, Phys. Rev. Lett. **100**, 103601 (2008).
- [9] K. Eckert *et al.*, Phys. Rev. Lett. **98**, 100404 (2007); K. Eckert *et al.*, Nature Phys. **4**, 50 (2008).
- [10] B. Mihaila *et al.*, Phys. Rev. A **74**, 063608 (2006).
- [11] R. W. Cherng and E. Demler, New J. Phys. **9**, 7 (2007).
- [12] D. Oblak *et al.*, Phys. Rev. A **71**, 043807 (2005).
- [13] M. W. Sørensen and A. S. Sørensen, Phys. Rev. A **77**, 013826 (2008).
- [14] I. Carusotto, J. Phys. B **39**, S211 (2006).
- [15] G. M. Bruun *et al.*, Eur. Phys. J. D **7**, 433 (1999).
- [16] Y. Shin *et al.*, Nature (London) **451**, 689 (2008).
- [17] S. Pilati and S. Giorgini, Phys. Rev. Lett. **100**, 030401 (2008).
- [18] We assume the laser does not probe the far edges of the gas where any spin imbalance exists as a normal phase.
- [19] G. M. Bruun and G. Baym, Phys. Rev. Lett. **93**, 150403 (2004); Phys. Rev. A **74**, 033623 (2006).
- [20] R. Jördens *et al.*, arXiv:0804.4009v1.
- [21] G. S. Rushbrooke, G. A. Baker, Jr., and P. J. Wood, in *Phase Transitions and Critical Phenomena*, edited by C. Domb and M. S. Green (Academic, London, 1974), Vol. 3, Chap. 5.
- [22] M. Takahashi, Phys. Rev. B **40**, 2494 (1989).
- [23] B. M. Andersen and G. M. Bruun, Phys. Rev. A **76**, 041602 (2007).
- [24] M. Snoek *et al.*, New J. Phys. **10**, 093008 (2008).
- [25] M. Hermele, T. Senthil, and M. P. A. Fisher, Phys. Rev. B **72**, 104404 (2005).
- [26] S. Peil *et al.*, Phys. Rev. A **67**, 051603 (2003).
- [27] A. W. Sandvik, Phys. Rev. Lett. **80**, 5196 (1998).